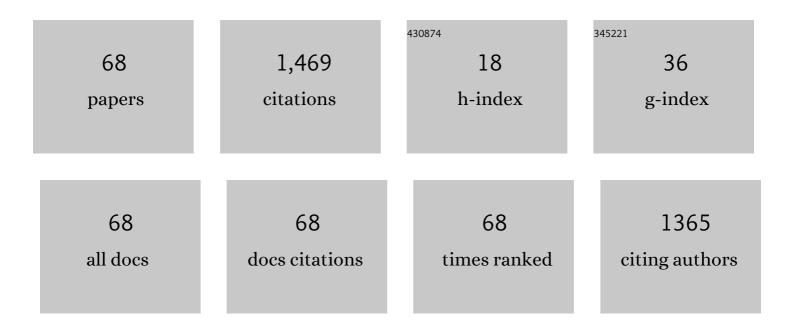


List of Publications by Year in descending order

Source: https://exaly.com/author-pdf/7689957/publications.pdf Version: 2024-02-01



VIKONC

#	Article	IF	CITATIONS
1	Simulation of a confined polymer in solution using the dissipative particle dynamics method. International Journal of Thermophysics, 1994, 15, 1093-1101.	2.1	143
2	Structural and elastic properties of cubic and hexagonal TiN and AlN from first-principles calculations. Computational Materials Science, 2010, 48, 705-709.	3.0	126
3	Extended Finnis–Sinclair potential for bcc and fcc metals and alloys. Journal of Physics Condensed Matter, 2006, 18, 4527-4542.	1.8	119
4	Interatomic potentials of the binary transition metal systems and some applications in materials physics. Physics Reports, 2008, 455, 1-134.	25.6	112
5	Quantified contribution of β″ and β′ precipitates to the strengthening of an aged Al–Mg–Si alloy. Materials Science & Engineering A: Structural Materials: Properties, Microstructure and Processing, 2020, 774, 138776.	5.6	84
6	Atomic scale investigation of the crystal structure and interfaces of the B′ precipitate in Al-Mg-Si alloys. Acta Materialia, 2020, 185, 193-203.	7.9	72
7	Atomic mobilities, diffusivities and simulation of diffusion growth in the Co–Si system. Acta Materialia, 2008, 56, 3940-3950.	7.9	69
8	Thermodynamic investigation of the galvanizing systems, I: Refinement of the thermodynamic description for the Fe–Zn system. Calphad: Computer Coupling of Phase Diagrams and Thermochemistry, 2009, 33, 433-440.	1.6	44
9	Long-range empirical potential for the bcc structured transition metals. Physical Review B, 2007, 75, .	3.2	43
10	Long-range empirical potential model: Application to fcc transition metals and alloys. Physical Review B, 2007, 75, .	3.2	43
11	Boosting charge transfer via molybdenum doping and electric-field effect in bismuth tungstate: Density function theory calculation and potential applications. Journal of Colloid and Interface Science, 2019, 534, 20-30.	9.4	36
12	Structure and thermodynamics of the key precipitated phases in the Al–Mg–Si alloys from first-principles calculations. Journal of Materials Science, 2011, 46, 7839-7849.	3.7	26
13	Structure, elastic and thermodynamic properties of the Ni–P system from first-principles calculations. Calphad: Computer Coupling of Phase Diagrams and Thermochemistry, 2011, 35, 284-291.	1.6	25
14	Structural evolution of oxygen on the surface of TiAlN: Ab initio molecular dynamics simulations. Applied Surface Science, 2019, 470, 520-525.	6.1	20
15	Effect of B-doping on the mechanical properties, thermal stability and oxidation resistance of TiAlN coatings. International Journal of Refractory Metals and Hard Materials, 2021, 98, 105531.	3.8	20
16	Native defects in LiNH <mml:math <br="" xmlns:mml="http://www.w3.org/1998/Math/MathML">display="inline"><mml:mrow><mml:msub><mml:mrow /><mml:mrow><mml:mn>2</mml:mn></mml:mrow></mml:mrow </mml:msub></mml:mrow></mml:math> : A first-principles study. Physical Review B, 2011, 84, .	3.2	19
17	Ab initio molecular dynamics studies on effect of Zr on oxidation resistance of TiAlN coatings. Applied Surface Science, 2016, 378, 293-300.	6.1	19
18	The effect of Ti atom on hydrogenation of Al(111) surface: First-principles studies. International Journal of Hydrogen Energy, 2010, 35, 609-613.	7.1	18

Υι Κονς

#	Article	IF	CITATIONS
19	Microstructure and composition of the grain/binder interface in WC–Ni3Al composites. International Journal of Refractory Metals and Hard Materials, 2014, 44, 88-93.	3.8	18
20	<mml:math <br="" xmlns:mml="http://www.w3.org/1998/Math/MathML">altimg="si2.svg"><mml:msup><mml:mrow><mml:mi>β</mml:mi></mml:mrow><mml:mrow><mml:mtext>'needle-shape precipitate formation in Al-Mg-Si alloy: Phase field simulation and experimental verification. Computational Materials Science, 2020, 184, 109878.</mml:mtext></mml:mrow></mml:msup></mml:math>	ml:mtext>	۰ <mml:mtext< td=""></mml:mtext<>
21	First-principles study of binary special quasirandom structures for the Al–Cu, Al–Si, Cu–Si, and Mg–Si systems. Calphad: Computer Coupling of Phase Diagrams and Thermochemistry, 2009, 33, 769-773.	1.6	17
22	Elastic and thermodynamic properties of the Ni–B system studied by first-principles calculations and experimental measurements. Calphad: Computer Coupling of Phase Diagrams and Thermochemistry, 2010, 34, 245-251.	1.6	15
23	Effect of diffusion barrier and interfacial strengthening on the interface behavior between high entropy alloy and diamond. Journal of Alloys and Compounds, 2021, 852, 157023.	5.5	15
24	The microstructural, mechanical and thermal properties of TiAlVN, TiAlSiN monolithic and TiAlVN/TiAlSiN multilayered coatings. Journal of Alloys and Compounds, 2022, 899, 163332.	5.5	15
25	Self-accommodated defect structures modifying the growth of Laves phase. Journal of Materials Science and Technology, 2021, 62, 203-213.	10.7	14
26	First-principles investigation on stability and electronic structure of Sc-doped Î,′/Al interface in Alâ^'Cu alloys. Transactions of Nonferrous Metals Society of China, 2021, 31, 3342-3355.	4.2	14
27	Strengthening mechanism of metallic nanoscale multilayer with negative enthalpy of mixing. Journal of Applied Physics, 2011, 110, .	2.5	13
28	Al–Pd interatomic potential and its application to nanoscale multilayer thin films. Materials Science & Engineering A: Structural Materials: Properties, Microstructure and Processing, 2011, 530, 73-86.	5.6	13
29	Self-Diffusion Coefficient of fcc Mg: First-Principles Calculations and Semi-Empirical Predictions. Journal of Phase Equilibria and Diffusion, 2011, 32, 128-137.	1.4	13
30	Microstructure, mechanical and thermal properties of TiAlTaN/TiAlSiN multilayer. Vacuum, 2021, 187, 110138.	3.5	13
31	Role of spatial valence charge density on the metastability of an immiscible binary metal system at equilibrium. Physical Review B, 2005, 72, .	3.2	12
32	First-Principles Calculation of the Structural, Magnetic, and Electronic Properties of the CoxCu1-x Solid Solutions Using Special Quasirandom Structures. Journal of the Physical Society of Japan, 2007, 76, 024605.	1.6	12
33	First-principles prediction of structural, mechanical and magnetic properties in Ni2MnAl. Computational Materials Science, 2016, 123, 52-58.	3.0	12
34	Atomic-scale study of compositional and structural evolution of early-stage grain boundary precipitation in Al–Cu alloys through phase-field crystal simulation. Journal of Materials Science, 2021, 56, 12700-12715.	3.7	12
35	Observation of magnetism in the nanoscale amorphous ruthenium clusters prepared by ion beam mixing. Applied Physics Letters, 2006, 89, 262511.	3.3	11
36	Proposed power-functionN-body potential for the fcc structured metals Ag, Au, Cu, Ni, Pd, and Pt. Physical Review B, 2007, 76, .	3.2	11

ΥΙ ΚΟΝG

#	Article	IF	CITATIONS
37	Spatial and electronic structure of the Ni3P surface. Applied Surface Science, 2010, 256, 7692-7695.	6.1	11
38	Thermodynamic modeling and solidified microstructure in the Mo–Nb–Zr ternary system. Calphad: Computer Coupling of Phase Diagrams and Thermochemistry, 2019, 66, 101630.	1.6	11
39	Construction ofn-body potentials for hcp-bcc metal systems within the framework of embedded atom method. Physical Review B, 2005, 71, .	3.2	10
40	Reassessment of the Ni–B system supported by key experiments and first-principles calculation. International Journal of Materials Research, 2009, 100, 59-67.	0.3	9
41	Interfacial effect on strengthening nanoscale metallic multilayers - a combined Hall-Petch relation and atomistic simulation study. Materials Science & Engineering A: Structural Materials: Properties, Microstructure and Processing, 2016, 663, 29-37.	5.6	9
42	Asymmetric mixing behavior and stability of the predicted phases in the W–Cu system. Calphad: Computer Coupling of Phase Diagrams and Thermochemistry, 2016, 53, 116-121.	1.6	9
43	Growth modes of grain boundary precipitate in aluminum alloys under different lattice misfits. Journal of Materials Science, 2022, 57, 2744-2757.	3.7	9
44	Positive correlation between the magnetic moment of Fe and atomic volume in the binary Fe–(Cu, Ag,) Tj ETQ	q0 0 0 rgE	BT /gverlock 10
45	Effect of stamping deformation on microstructure and properties evolution of an Al–Mg–Si–Cu alloy for automotive panels. Journal of Materials Science, 2017, 52, 5569-5581.	3.7	8
46	Impact of oxygen content on the thermal stability of Ti-Al-O-N coatings based on computational and experimental studies. Acta Materialia, 2022, 227, 117706.	7.9	8
47	Calculation of phonon spectra to predict the high-pressure metastable phase in an equilibrium immiscible Cu–Ta system. Applied Physics Letters, 2004, 85, 1517-1519.	3.3	7
48	First-principles calculations of the structural stability and magnetic property of the metastable phases in the equilibrium immiscible Co–Au system. Journal of Physics Condensed Matter, 2006, 18, 4345-4353.	1.8	7
49	Thermodynamic Assessment of the Cu-B System Supported by Key Experiment and First-Principles Calculations. Journal of Phase Equilibria and Diffusion, 2009, 30, 480-486.	1.4	7

50Energetic, mechanical, and vibrational stability of metastable OsC phase. Journal of Applied Physics,
2010, 108, .2.57

51Nano/micro mechanics study of nanoindentation on thin Al/Pd films. Journal of Materials Research,
2015, 30, 699-708.2.6752Effect of electron beam irradiation in TEM on the microstructure and composition of
nanoprecipitates in Al-Mg-Si alloys. Micron, 2019, 116, 116-123.2.27

52Effect of alloying on stability of grain boundary in γ phase of the U–Mo and U–Nb systems. Calphad:
Computer Coupling of Phase Diagrams and Thermochemistry, 2021, 72, 102241.2.27

⁵⁴ Mechanical properties of $\hat{l}^2 \hat{a} \in 3$ precipitates containing Al and/or Cu in age hardening Al alloys. Journal of Materials Research, 2016, 31, 580-588. 2.6 6

Υι Κονς

#	Article	IF	CITATIONS
55	Phase field crystal simulation of the structure evolution between the hexagonal and square phases at elevated pressures. Journal of Mining and Metallurgy, Section B: Metallurgy, 2017, 53, 271-278.	0.8	6
56	Nonequilibrium Solid Phase Formation Studied by Lattice Dynamics Calculation and Ion Beam Mixing in an Immiscible Coâ^Ag System. Journal of Physical Chemistry B, 2005, 109, 9362-9367.	2.6	5
57	The microstructure evolution of U1 and U2 nanowires constrained in Al matrix. Computational Materials Science, 2016, 117, 180-187.	3.0	4
58	Unusual Force Constants Guided Distortion-Triggered Loss of Long-Range Order in Phase Change Materials. Materials, 2021, 14, 3514.	2.9	4
59	Discovery of a bulk C36-type MgZn2 structure step by step transformed from the C14 prototype laves phase structure. Journal of Materials Science, 2022, 57, 2999-3009.	3.7	4
60	Atomic site occupancy of alloying elements and Laves phase stability in γ-γ′ Co-base superalloys. Journal of Alloys and Compounds, 2022, 906, 164261.	5.5	4
61	Oscillating behavior of high-pressure stability observed in the immiscible Co–Cu system by first-principles calculation. Journal of Applied Physics, 2007, 101, 056102.	2.5	3
62	A First-Principles Study of the Cu-Containing β″ Precipitates in Al-Mg-Si-Cu Alloy. Materials, 2021, 14, 7879.	2.9	2
63	Cage-like structure and charge hollow in the immiscible Cu–Ta system. Solid State Communications, 2009, 149, 1974-1977.	1.9	1
64	Structural stability of high-pressure phase in the immiscible Cu–Nb system studied by lattice dynamics calculation. Journal of Alloys and Compounds, 2009, 468, 299-302.	5.5	1
65	COMPARISON OF EQUATION OF STATE AND THE FOUR-PARAMETER < font > Li < /font > EQUATION OF STATE IN ALLOY. Modern Physics Letters B, 2011, 25, 1557-1568.	1.9	1
66	Three-dimensional phase field simulation for rafting of multiparticle precipitate in elastic inhomogeneous alloy under external stress. Journal of Mining and Metallurgy, Section B: Metallurgy, 2019, 55, 101-110.	0.8	1
67	Nonequilibrium Solid Phase Formation Studied by Lattice Dynamics Calculation and Ion Beam Mixing in an Immiscible Co—Ag System ChemInform, 2005, 36, no.	0.0	0
68	Developing Cemented Carbides Through ICME. Minerals, Metals and Materials Series, 2017, , 155-167.	0.4	0